Frontiers of Information Technology & Electronic Engineering
www.zju.edu.cn/jzus; engineering.cae.cn; www.springerlink.com
ISSN 2095-9184 (print); ISSN 2095-9230 (online)
E-mail: jzus@zju.edu.cn

Joint cooperative beamforming and artificial noise design for secure AF relay networks with energy-harvesting eavesdroppers*

He-hao NIU[†], Bang-ning ZHANG[†‡], Dao-xing GUO, Yu-zhen HUANG, Ming-yue LU

(*College of Communications Engineering, PLA University of Science and Technology, Nanjing 210007, China*)

[†]E-mail: niuhaonupt@foxmail.com; zbnlgdx2015@sina.com

Received Dec. 20, 2016; Revision accepted Apr. 30, 2017; Crosschecked May 15, 2017

Abstract: In this paper, we investigate physical layer security for simultaneous wireless information and power transfer in amplify-and-forward relay networks. We propose a joint robust cooperative beamforming and artificial noise scheme for secure communication and efficient wireless energy transfer. Specifically, by treating the energy receiver as a potential eavesdropper and assuming that only imperfect channel state information can be obtained, we formulate an optimization problem to maximize the worst-case secrecy rate between the source and the legitimate information receiver under both the power constraint at the relays and the wireless power harvest constraint at the energy receiver. Since such a problem is non-convex and hard to tackle, we propose a two-level optimization approach which involves a one-dimensional search and semidefinite relaxation. Simulation results show that the proposed robust scheme achieves better worst-case secrecy rate performance than other schemes.

Key words: Simultaneous wireless information and power transfer; Physical layer security; Relay networks; Cooperative beamforming; Artificial noise

http://dx.doi.org/10.1631/FITEE.1601832 **CLC number:** TN911.7

1 Introduction

With the rapid development of mobile devices and base stations, the telecommunication industry annually causes a significant carbon emission. As a result, the green aspect is the utmost concern in fifth generation (5G) mobile communication systems (Andrews *et al.*, 2014). Recently, a novel technology, energy harvesting (EH), has been proposed for the 5G systems to circumvent the issue of energy limitations in mobile devices and improve the energy efficiency of the networks by extracting energy from the external natural environment (Yuen *et al.*, 2015a; 2015b; 2015c).

Traditionally, energy is directly harvested from external sources without exploiting the resources of the communication network itself. However, when the natural environment is not able to provide stable energy, wireless mobile receivers have to find an alternative energy source, which can be the information-carrying radio frequency (RF) signal radiated by fixed transmitters (base station, hot spots, etc.) (Krikidis *et al.*, 2014). Some recent results have shown that information and energy can be carried by the same RF signal simultaneously, termed 'simultaneous wireless information and power transfer (SWIPT)' (Zhang and Ho, 2013; Huang *et al.*, 2014; Xu *et al.*, 2014; Wang *et al.*, 2016a; 2016b).

‡ Corresponding author

* Project supported by the National Natural Science Foundation of China (No. 61501507), the Jiangsu Provincial Natural Science Foundation of China (No. BK20150719), and the China Postdoctoral Science Foundation (No. 2017M610066)

ORCID: He-hao NIU, http://orcid.org/0000-0002-6423-3482

SWIPT has been studied for various communication systems in different contexts. Specifically, Xu *et al.* (2014) investigated the optimal information and energy beamforming strategy for the multiuser multiple-input single-output (MISO) SWIPT system. Zhang and Ho (2013) considered the beamforming scheme in a multiple-input multiple-output (MIMO) broadcast system and demonstrated that beamforming can control the transmission directions of information and power effectively. Huang *et al.* (2014) investigated the beamforming scheme of SWIPT in a half-duplex relay system. Wang *et al.* (2016a) investigated the SWIPT design in a full-duplex relay system, where the signals received at the relay are split according to a power splitting (PS) ratio for information processing and EH. Later, the work in Wang *et al.* (2016a) was extended in Wang *et al.* (2016b) with two-way full-duplex relay systems being considered.

On the other hand, transmitting energy and information simultaneously makes the system vulnerable to security attacks, since the message sent to the legitimate information receiver (IR) can be eavesdropped by other nodes. This is an important problem in 5G systems (Yang *et al.*, 2015). Chen *et al.* (2016) proposed the physical layer security (PLS) technique to exploit the characteristics of wireless channels (such as fading and interference (Zhang R *et al.*, 2016)) to improve the security of the SWIPT system. This technique has been considered as a promising solution in many senarios (Liu *et al.*, 2013; Feng *et al.*, 2015; Khandaker and Wong, 2015a; 2015b; Shi *et al.*, 2015; Tian *et al.*, 2015; Wang SH and Wang BY, 2015; Chu *et al.*, 2016; Xing *et al.*, 2016). Specifically, the problem of secure SWIPT in a single-input single-output (SISO) fading wiretap channel was investigated by Xing *et al.* (2016). Liu *et al.* (2013) investigated the secure beamforming technique in a MISO SWIPT system. Later, the system model in Liu *et al.* (2013) was extended to the MIMO system in Shi *et al.* (2015), where multiple data streams were transmitted in parallel through spatial multiplexing to improve the achievable secrecy rate. Among the techniques in the literature, reducing the artificial noise (AN) is an effective way to improve the security performance. It can reinforce the signals received at both IR and the energy receiver (ER) while degrading the signals received at the eavesdropper.

Note that all these works assume that perfect knowledge of eavesdropper's channel state information (CSI) can be obtained. In practice, it may be difficult to obtain the CSI of the link between the transmitter and the eavesdropper due to channel estimation and quantization errors. To handle this issue, robust optimization techniques have been introduced by Feng *et al.*, (2015), Khandaker and Wong (2015a; 2015b), Tian *et al.* (2015), Wang SH and Wang BY (2015), and Chu *et al.* (2016). Specifically, robust secure beamforming schemes for a MISO SWIPT system were investigated with AN (Tian *et al.*, 2015) or without AN (Feng *et al.*, 2015). Among these works, the worst-case secrecy rate maximization (WCSRM) criterion has been widely applied to formulate the optimization problem.

All the above works have been focused on the scenario in which ER and the eavesdropper are geometrically separated, while several works investigated the scenario of co-located ER and eavesdropper, e.g., treating ER as a potential eavesdropper. Specifically, the robust secure power minimization in the MISO downlink channel with single-antenna ERs was investigated by Khandaker and Wong (2015b). Khandaker and Wong (2015a) investigated the WCSRM problem for the MISO channel considering multiple colluding ERs. Recently, Chu *et al.* (2016) investigated the WCSRM problem for the MISO downlink channel in the presence of multi-antenna ERs, and proposed a joint robust design of the transmit beamforming vector, AN, and the PS ratio. Wang SH and Wang BY (2015) investigated a joint robust precoding, AN, and the PS scheme in the MIMO system, and proposed a suboptimal algorithm based on the Taylor series expansion.

Cooperative relaying is a popular approach for extending network coverage and providing spatial degrees of freedom (DoF), beneficial to improve PLS (Rodriguez *et al.*, 2015). Cooperative methods, such as cooperative beamforming (CB) and cooperative jamming (CJ), have been widely investigated in the literature (Li *et al.*, 2011; Zhang *et al.*, 2012; Yang *et al.*, 2013a; 2013b; Li *et al.*, 2015; Wang C and Wang HM, 2015). Specifically, Li *et al.* (2011) investigated BC and CJ for decode-and-forword (DF) relay. It is more difficult to design the CB vector in amplify-and-forward (AF) relay networks due to the effect of noise amplification. Zhang *et al.* (2012) investigated the PLS design for the untrusted AF relay in the presence of friendly jammers. Yang *et al.* (2013a) proposed a suboptimal design, where the information is transmitted in the null space of the relay-eavesdroppers channels. However, the design is limited to the scenario where the number of eavesdroppers is smaller than the number of relays. To take advantage of the available DoF at the relays, a joint CB and AN (CBAN) scheme was proposed by Yang *et al.* (2013b). For the scenario of imperfect eavesdropper CSI, a joint robust design of the CB and CJ scheme for the AF relay network was proposed by Wang C and Wang HM (2015) for multiple multi-antenna eavesdroppers based on an iterative optimization algorithm. Li *et al.* (2015) investigated the joint robust design of the AF beamforming matrices and the AN covariance matrices in the scenario of multiple multi-antenna AF relays, which can be seen as a generalization of the work in Wang C and Wang HM (2015).

Recently, secure transmission in the SWIPT relay system has aroused great concerns (Li *et al.*, 2014; 2016; Son and Kong, 2015; Xing *et al.*, 2015; Salem *et al.*, 2016; Zhang G *et al.*, 2016; Feng *et al.*, 2017). Specifically, Xing *et al.* (2015) investigated the secrecy rate maximization (SRM) problem in the EH-enabled AF relay wiretap channels. Son and Kong (2015) proposed a cooperative transmission scheme in an EH-enabled AF relay system with an eavesdropper. Salem *et al.* (2016) analyzed the secrecy capacity of a half-duplex EH-based multi-antenna AF relay network in the presence of an eavesdropper. Li *et al.* (2014) investigated the SRM problem subject to the relay power budget and the EH constraints. Different from Li *et al.* (2014), Li *et al.* (2016) considered a two-way AF relay network and proposed a null space based CBAN scheme, which is a simple but suboptimal strategy. Zhang G *et al.* (2016) investigated a joint design of the signal AN beamforming at the source, and AF beamforming at the relay. Feng *et al.* (2017) proposed a joint CB and energy signal (ES) scheme for secure SWIPT in the AF relay wiretap channel.

Motivated by these works, in this paper, we investigate the PLS for SWIPT in AF relay networks. Specifically, we focus on the following settings: (1) Multiple single-antenna relays cooperatively forward information from the source to a legitimate IR in the presence of multiple multi-antenna ERs, which may act as potential eavesdroppers; (2) Relays employ the CBAN scheme to fulfill secure communication and meet the EH requirement for ER; (3) Relays have perfect CSI of IR, but imperfect CSI of ER; (4) Relays are subjected to both total and individual power constraints. Based on these settings, we formulate the WCSRM problem and propose a two-level optimization method to solve it. In the proposed method, the outer problem is tackled by a one-dimensional search and the inner one can be efficiently solved by semidefinite relaxation (SDR) (Luo *et al.*, 2010) and S-procedure (Luo *et al.*, 2004). In addition, with the help of Karush-Kuhn-Tucker (KKT) optimality, the tightness of SDR is established.

One of the most related works is Feng *et al.* (2017). However, the differences between Feng *et al.* (2017) and our work are summarized as follows: First, we consider the scenario of co-located ER and eavesdropper (e.g., we treat ER as a potential eavesdropper), while Feng *et al.* (2017) investigated the case of an individual ER and eavesdropper. Second, we consider AN rather than the ES method proposed by Feng *et al.* (2017), who assumed that a pseudo-random ES is priori known at IR but not at the eavesdroppers, and can be totally cancellated at IR, which is overly optimistic because, for the total cancellation of the ES at IR, we need to exchange the secret key and use the reciprocity of the channels between the transmitter and the IR. Feng *et al.* (2017) considered the case of multiple single-antenna colluding eavesdroppers, since the colluding of multiple single-antenna eavesdroppers can be mathematically equivalent to that of a multi-antenna eavesdropper (Wang C and Wang HM, 2015; Feng *et al.*, 2017); hence, the work in Feng *et al.* (2017) can be seen as a special case of our work.

Notations: Throughout the paper, we use the uppercase boldface letters for matrices and lowercase boldface letters for vectors. The superscripts $(\cdot)^{\mathrm{T}}$, $(\cdot)^{\dagger}$, and $(\cdot)^{\mathrm{H}}$ represent transpose, conjugate, and conjugate transpose, respectively. The trace and rank of matrix $\boldsymbol{A}$ are denoted as $\mathrm{tr}(\boldsymbol{A})$ and $\mathrm{rank}(\boldsymbol{A})$, respectively. $\boldsymbol{a} = \mathrm{vec}(\boldsymbol{A})$ denotes stacking the columns of matrix $\boldsymbol{A}$ into a vector $\boldsymbol{a}$. $\mathrm{vec}^{-1}(\cdot)$ is the inverse operation of $\mathrm{vec}(\cdot)$. $\boldsymbol{A} \succeq 0$ indicates that $\boldsymbol{A}$ is a positive semi-definite matrix. $|\cdot|$, $\|\cdot\|$, $\|\cdot\|_{\mathrm{F}}$, $\otimes$, and $\odot$ represent the absolute value, Euclidean norm, Frobenius norm, Kronecker product, and Hadamard product, respectively. $\boldsymbol{D}(\boldsymbol{a})$

represents a diagonal matrix with $\boldsymbol{a}$ on the main diagonal. $\boldsymbol{I}$ denotes an identity matrix with an appropriate size. $\mathrm{Re}\{a\}$ denotes the real part of a complex variable a. $\mathcal{CN}(\mathbf{0}, \boldsymbol{I})$ denotes a circularly symmetric complex Gaussian random vector with mean $\mathbf{0}$ and covariance matrix $\boldsymbol{I}$. $[x]^+$ indicates $\max(0, x)$. $\lambda_{\min}(\boldsymbol{A}, \boldsymbol{B})$ denotes the minimum generalized eigenvalue of matrices $\boldsymbol{A}$ and $\boldsymbol{B}$. $\mathbb{E}[\cdot]$ stands for statistical expectation.

2 System model and problem statement

2.1 System model

We consider a cooperative relay wiretap channel for SWIPT (Fig. 1), in which a transmitter sends confidential messages to IR while transferring wireless energy to M ERs, with the aid of K AF relays. We assume that each ER is equipped with N_e antennas while the others are each equipped with a single antenna. Let $\boldsymbol{f} \in \mathbb{C}^{K\times 1}$, $\boldsymbol{h} \in \mathbb{C}^{K\times 1}$, and $\boldsymbol{G}_m \in \mathbb{C}^{K\times N_\mathrm{e}}$ denote the channel responses from the transmitter to the relays, the relays to IR, and the relays to the mth ER, respectively. We assume that the channels between the transmitter and the relays are perfectly known and there is no direct link between the transmitter and IR or ERs, which is a common assumption in the literature (Li *et al.*, 2014; Zhang G *et al.*, 2016; Feng *et al.*, 2017). Since the relays operate in a half-duplex mode, one transmission round is composed of two phases.

In the first phase, the transmitter broadcasts its information s satisfying $\mathbb{E}[|s|^2] = 1$ to the relays.

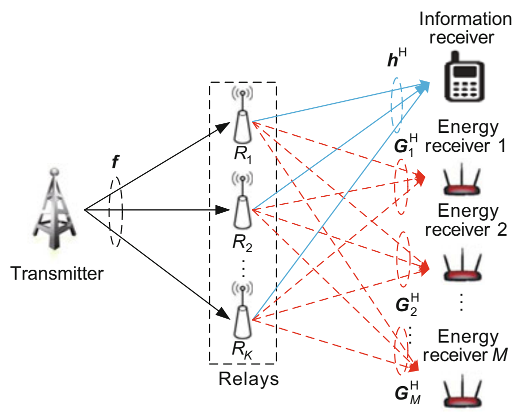

Fig. 1 System model for secure simultaneous wireless information and power transfer in the amplify-and-forward relay network

The received signal at the relays is given by

$$\boldsymbol{y}_\mathrm{r} = [\boldsymbol{y}_{\mathrm{r},1}, \boldsymbol{y}_{\mathrm{r},2}, \cdots, \boldsymbol{y}_{\mathrm{r},K}]^\mathrm{T} = \sqrt{P_\mathrm{s}}\boldsymbol{f}s + \boldsymbol{n}_\mathrm{r}, \tag{1}$$

where P_s is the transmit power at the transmitter and $\boldsymbol{n}_\mathrm{r}$ is the additive noise at the relays with distribution $\mathcal{CN}(\mathbf{0}, \sigma_\mathrm{r}^2\boldsymbol{I})$.

In the second phase, the relays employ the cooperative beamforming vector $\boldsymbol{w} \in \mathbb{C}^{K\times 1}$ to forward the source information and emit artificial noise $\boldsymbol{z} \in \mathbb{C}^{K\times 1}$ with distribution $\mathcal{CN}(\mathbf{0}, \boldsymbol{Q})$. Thus, the signal transmitted by the relays is given by

$$\boldsymbol{x}_\mathrm{r} = \boldsymbol{D}(\boldsymbol{y}_\mathrm{r})\boldsymbol{w} + \boldsymbol{z}. \tag{2}$$

The signals received at IR and the mth ER are respectively given by

$$\boldsymbol{y}_\mathrm{I} = \sqrt{P_\mathrm{s}}\boldsymbol{h}^\mathrm{H}\boldsymbol{D}(\boldsymbol{f})\boldsymbol{w}s + \boldsymbol{h}^\mathrm{H}\boldsymbol{D}(\boldsymbol{w})\boldsymbol{n}_\mathrm{r} + \boldsymbol{h}^\mathrm{H}\boldsymbol{z} + \boldsymbol{n}_\mathrm{I}, \tag{3a}$$

$$\boldsymbol{y}_m = \sqrt{P_\mathrm{s}}\boldsymbol{G}_m^\mathrm{H}\boldsymbol{D}(\boldsymbol{f})\boldsymbol{w}s + \boldsymbol{G}_m^\mathrm{H}\boldsymbol{D}(\boldsymbol{w})\boldsymbol{n}_\mathrm{r} + \boldsymbol{G}_m^\mathrm{H}\boldsymbol{z} + \boldsymbol{n}_m, \tag{3b}$$

where $\boldsymbol{n}_\mathrm{I}$ and $\boldsymbol{n}_m$ are additive noises at IR and the mth ER, respectively, both with a variance σ_I^2 and $\mathcal{CN}(\mathbf{0}, \sigma_m^2\boldsymbol{I})$.

For the received signal model (3), given $\boldsymbol{w}$ and $\boldsymbol{Q}$, the achievable information rates of IR and the mth ER are

$$C_\mathrm{I}(\boldsymbol{w}, \boldsymbol{Q}) = \log_2\left(1 + \frac{\boldsymbol{w}^\mathrm{H}\boldsymbol{A}\boldsymbol{w}}{\sigma_\mathrm{I}^2 + \boldsymbol{w}^\mathrm{H}\boldsymbol{B}\boldsymbol{w} + \boldsymbol{h}^\mathrm{H}\boldsymbol{Q}\boldsymbol{h}}\right), \tag{4a}$$

$$C_m(\boldsymbol{w}, \boldsymbol{Q}) = \log_2\left(1 + P_\mathrm{s}\left(\boldsymbol{G}_m^\mathrm{H}\boldsymbol{F}\boldsymbol{w}\right)^\mathrm{H}\boldsymbol{R}_m^{-1}\left(\boldsymbol{G}_m^\mathrm{H}\boldsymbol{F}\boldsymbol{w}\right)\right), \tag{4b}$$

respectively, where $\boldsymbol{A} = P_\mathrm{s}\boldsymbol{D}^\mathrm{H}(\boldsymbol{f})\boldsymbol{h}\boldsymbol{h}^\mathrm{H}\boldsymbol{D}(\boldsymbol{f})$, $\boldsymbol{B} = \sigma_\mathrm{r}^2\boldsymbol{D}(\boldsymbol{h})\boldsymbol{D}^\mathrm{H}(\boldsymbol{h})$, $\boldsymbol{F} = \boldsymbol{D}(\boldsymbol{f})$, and

$$\boldsymbol{R}_m = \sigma_m^2\boldsymbol{I} + \sigma_\mathrm{r}^2\boldsymbol{G}_m^\mathrm{H}\boldsymbol{W}\boldsymbol{W}^\mathrm{H}\boldsymbol{G}_m + \boldsymbol{G}_m^\mathrm{H}\boldsymbol{Q}\boldsymbol{G}_m, \tag{5}$$

with $\boldsymbol{W} = \boldsymbol{D}(\boldsymbol{w})$.

By neglecting the noise power, the harvest energy at the mth ER (normalized by the baseband symbol duration) can be expressed as

$$\begin{aligned} &E_m(\boldsymbol{w}, \boldsymbol{Q}) \\ &= \rho_m \mathrm{tr}(\boldsymbol{G}_m^\mathrm{H}(P_\mathrm{s}\boldsymbol{F}\boldsymbol{w}\boldsymbol{w}^\mathrm{H}\boldsymbol{F}^\mathrm{H} + \sigma_\mathrm{r}^2\boldsymbol{W}\boldsymbol{W}^\mathrm{H} + \boldsymbol{Q})\boldsymbol{G}_m), \end{aligned} \tag{6}$$

where $0 \le \rho_m \le 1$ denotes the energy transfer efficiency for the mth ER.

2.2 Problem statement

In this study, we assume that only imperfect ERs' CSI can be obtained. We use a deterministic spherical model (Feng *et al.*, 2015; Khandaker and Wong, 2015a; 2015b; Li *et al.*, 2015; Tian *et al.*, 2015; Wang C and Wang HM, 2015; Wang SH and Wang BY, 2015; Chu *et al.*, 2016) to characterize the CSI's uncertainties as

$$\mathcal{G}_m = \left\{\boldsymbol{G}_m \left| \boldsymbol{G}_m = \bar{\boldsymbol{G}}_m + \Delta\boldsymbol{G}_m, \|\Delta\boldsymbol{G}_m\|_{\mathrm{F}} \le \varepsilon_m \right.\right\}, \quad \forall m, \tag{7}$$

where $\bar{\boldsymbol{G}}_m$ denotes the estimate of the respective CSI, $\Delta\boldsymbol{G}_m$ denotes their respective error, and ε_m represents the respective size of the bounded error region.

Based on the system model, the worst-case secrecy rate is given by

$$R_{\mathrm{s}} = \left[\frac{1}{2} \min_{\forall \boldsymbol{G}_m \in \mathcal{G}_m, \forall m} \{C_{\mathrm{I}}(\boldsymbol{w},\boldsymbol{Q}) - C_m(\boldsymbol{w},\boldsymbol{Q})\}\right]^+. \tag{8}$$

Our interest is to maximize the worst-case secrecy rate while transferring a certain amount of energy to ERs by jointly designing the CB vector $\boldsymbol{w}$ and AN covariance $\boldsymbol{Q}$. Mathematically, it can be modeled as

$$\max_{\boldsymbol{w},\boldsymbol{Q}\succeq 0} \ \frac{1}{2}\left\{C_{\mathrm{I}}(\boldsymbol{w},\boldsymbol{Q}) - \max_{\forall \boldsymbol{G}_m \in \mathcal{G}_m, \forall m} C_m(\boldsymbol{w},\boldsymbol{Q})\right\} \tag{9a}$$

$$\text{s.t.} \quad E_m(\boldsymbol{w},\boldsymbol{Q}) \ge \eta_m, \forall \boldsymbol{G}_m \in \mathcal{G}_m, \forall m, \tag{9b}$$

$$\mathrm{tr}(\boldsymbol{C}\boldsymbol{w}\boldsymbol{w}^{\mathrm{H}} + \boldsymbol{Q}) \le P_{\mathrm{r}}, \tag{9c}$$

$$\mathrm{tr}((\boldsymbol{C}\boldsymbol{w}\boldsymbol{w}^{\mathrm{H}} + \boldsymbol{Q})\boldsymbol{e}_k\boldsymbol{e}_k^{\mathrm{H}}) \le P_k, \forall k, \tag{9d}$$

where $\boldsymbol{C} = P_{\mathrm{s}}\boldsymbol{F}^{\mathrm{H}}\boldsymbol{F} + \sigma_{\mathrm{r}}^2\boldsymbol{I}$, P_{r} and P_k denote the total and individual power budgets at the relays, respectively, and $\boldsymbol{e}_k$ is a $K \times 1$ unit vector with the kth entry being equal to one.

It is highlighted that problem (9) is a non-convex semi-infinite optimization problem. In the next section, we will develop a tractable solution to problem (9) through convex relaxation.

3 Joint robust cooperative beamforming and artificial noise design

In this section, we will first reformulate problem (9) into a two-level optimization problem, and then show that it can be handled by solving a sequence of convex optimization problems.

3.1 A single variable reformation of problem (9)

Let us introduce a slack variable β and rewrite problem (9) as

$$\max_{\boldsymbol{w},\boldsymbol{Q}\succeq 0,\beta} \frac{1}{2}C_{\mathrm{I}}(\boldsymbol{w},\boldsymbol{Q}) - \frac{1}{2}\log_2\left(\frac{1}{\beta}\right) \tag{10a}$$

$$\text{s.t.} \max_{\boldsymbol{G}_m \in \mathcal{G}_m} C_m(\boldsymbol{w},\boldsymbol{Q}) \le \log_2\left(\frac{1}{\beta}\right), \forall m, \tag{10b}$$

$$\text{constraints (9b)–(9d).} \tag{10c}$$

By following a similar method in Li *et al.* (2015), problem (10) can be equivalently formulated as a two-level optimization problem, where the outer level is a single-variable optimization problem with respect to (w.r.t.) β, i.e.,

$$R_{\mathrm{s}}^{\star} = \max_{\beta} \ \frac{1}{2}\log_2(\beta + \gamma(\beta)) \tag{11a}$$

$$\text{s.t.} \ \beta_{\min} \le \beta \le 1, \tag{11b}$$

and the inner part is a quadratic fractional problem w.r.t. $\boldsymbol{w}$ and $\boldsymbol{Q}$ for a fixed β, formulated as

$$\gamma(\beta) \triangleq \max_{\boldsymbol{w},\boldsymbol{Q}\succeq 0} \ \frac{\boldsymbol{w}^{\mathrm{H}}\boldsymbol{A}\boldsymbol{w}}{\beta^{-1}(\sigma_{\mathrm{I}}^2 + \boldsymbol{w}^{\mathrm{H}}\boldsymbol{B}\boldsymbol{w} + \boldsymbol{h}^{\mathrm{H}}\boldsymbol{Q}\boldsymbol{h})} \tag{12a}$$

$$\text{s.t.} \ P_{\mathrm{s}}\left(\boldsymbol{G}_m^{\mathrm{H}}\boldsymbol{F}\boldsymbol{w}\right)^{\mathrm{H}}\boldsymbol{R}_m^{-1}\left(\boldsymbol{G}_m^{\mathrm{H}}\boldsymbol{F}\boldsymbol{w}\right) \le \frac{1}{\beta} - 1, \quad \forall \boldsymbol{G}_m \in \mathcal{G}_m, \forall m, \tag{12b}$$

$$\text{constraints (9b)–(9d).} \tag{12c}$$

The lower bound $\beta_{\min}$ is derived as follows:

$$\begin{aligned}\beta &\ge \left(1 + \frac{\boldsymbol{w}^{\mathrm{H}}\boldsymbol{A}\boldsymbol{w}}{\sigma_{\mathrm{I}}^2 + \boldsymbol{w}^{\mathrm{H}}\boldsymbol{B}\boldsymbol{w} + \boldsymbol{h}^{\mathrm{H}}\boldsymbol{Q}\boldsymbol{h}}\right)^{-1} \\ &\ge \left(1 + \frac{\boldsymbol{w}^{\mathrm{H}}\boldsymbol{A}\boldsymbol{w}}{\boldsymbol{w}^{\mathrm{H}}\boldsymbol{B}\boldsymbol{w}}\right)^{-1} = \frac{\boldsymbol{w}^{\mathrm{H}}\boldsymbol{B}\boldsymbol{w}}{\boldsymbol{w}^{\mathrm{H}}(\boldsymbol{A}+\boldsymbol{B})\boldsymbol{w}} \\ &\ge \lambda_{\min}((\boldsymbol{A}+\boldsymbol{B}),\boldsymbol{B}) \triangleq \beta_{\min} > 0.\end{aligned} \tag{13}$$

Note that the outer-level problem (11) is a single-variable optimization problem, which can be solved by performing a one-dimensional line search over β. However, the inner-level problem (12) is still non-convex. In what follows, we focus on solving problem (12) by developing an SDR approach.

3.2 A semidefinite relaxation approach to problem (12)

As a standard routine of SDR, let us denote $\boldsymbol{\mathcal{W}} \triangleq \boldsymbol{w}\boldsymbol{w}^{\mathrm{H}}$, which means $\boldsymbol{\mathcal{W}} \succeq 0$ and $\mathrm{rank}(\boldsymbol{\mathcal{W}}) = 1$.

To reformulate problem (12) into an SDP problem w.r.t. $\boldsymbol{\mathcal{W}}$, we need to do some manipulation to the constraints in problem (12).

First, by applying Schur's complement (Boyd and Vandenberghe, 2004) to the right-hand side of constraint (12b), we have

$$\begin{aligned} & P_{\mathrm{s}}(\boldsymbol{G}_m^{\mathrm{H}}\boldsymbol{F}\boldsymbol{w})^{\mathrm{H}}\boldsymbol{R}_m^{-1}(\boldsymbol{G}_m^{\mathrm{H}}\boldsymbol{F}\boldsymbol{w}) \le \frac{1}{\beta}-1 \\ \Leftrightarrow & \begin{bmatrix} \frac{\beta^{-1}-1}{P_{\mathrm{s}}} & (\boldsymbol{G}_m^{\mathrm{H}}\boldsymbol{F}\boldsymbol{w})^{\mathrm{H}} \\ \boldsymbol{G}_m^{\mathrm{H}}\boldsymbol{F}\boldsymbol{w} & \boldsymbol{R}_m \end{bmatrix} \succeq 0 \\ \Leftrightarrow & \boldsymbol{R}_m \succeq \frac{P_{\mathrm{s}}}{\beta^{-1}-1}\boldsymbol{G}_m^{\mathrm{H}}\boldsymbol{F}\boldsymbol{w}(\boldsymbol{G}_m^{\mathrm{H}}\boldsymbol{F}\boldsymbol{w})^{\mathrm{H}}. \end{aligned} \tag{14}$$

Substituting $\boldsymbol{R}_m$ in Eq. (5) into Eq. (14), problem (14) can be equivalently rewritten as

$$\boldsymbol{G}_m^{\mathrm{H}}\boldsymbol{\varPsi}(\boldsymbol{\mathcal{W}},\boldsymbol{Q},\beta)\boldsymbol{G}_m+\sigma_m^2\boldsymbol{I}\succeq 0, \forall \boldsymbol{G}_m\in\mathcal{G}_m, \tag{15}$$

where

$$\boldsymbol{\varPsi}(\boldsymbol{\mathcal{W}},\boldsymbol{Q},\beta)\triangleq\sigma_{\mathrm{r}}^2\boldsymbol{\mathcal{W}}\odot\boldsymbol{I}-\frac{P_{\mathrm{s}}}{\beta^{-1}-1}\boldsymbol{F}\boldsymbol{\mathcal{W}}\boldsymbol{F}^{\mathrm{H}}+\boldsymbol{Q}. \tag{16}$$

Similarly, constraint (9b) can be equivalently rewritten as

$$\rho_m\mathrm{tr}(\boldsymbol{G}_m^{\mathrm{H}}\boldsymbol{\varGamma}(\boldsymbol{\mathcal{W}},\boldsymbol{Q})\boldsymbol{G}_m)\ge\eta_m,\forall\boldsymbol{G}_m\in\mathcal{G}_m,\forall m, \tag{17}$$

where

$$\boldsymbol{\varGamma}(\boldsymbol{\mathcal{W}},\boldsymbol{Q})\triangleq\sigma_{\mathrm{r}}^2\boldsymbol{\mathcal{W}}\odot\boldsymbol{I}+P_{\mathrm{s}}\boldsymbol{F}\boldsymbol{\mathcal{W}}\boldsymbol{F}^{\mathrm{H}}+\boldsymbol{Q}. \tag{18}$$

Combining these relationships and neglecting the non-convex constraint $\mathrm{rank}(\boldsymbol{\mathcal{W}})=1$, we obtain the following SDR problem:

$$\begin{aligned} &\gamma_{\mathrm{relax}}(\beta)\triangleq \\ &\max_{\boldsymbol{\mathcal{W}}\succeq 0,\boldsymbol{Q}\succeq 0}\ \frac{\mathrm{tr}(\boldsymbol{A}\boldsymbol{\mathcal{W}})}{\beta^{-1}(\sigma_{\mathrm{I}}^2+\mathrm{tr}(\boldsymbol{B}\boldsymbol{\mathcal{W}}+\boldsymbol{h}\boldsymbol{h}^{\mathrm{H}}\boldsymbol{Q}))} && \text{(19a)}\\ &\text{s.t. } \boldsymbol{G}_m^{\mathrm{H}}\boldsymbol{\varPsi}(\boldsymbol{\mathcal{W}},\boldsymbol{Q},\beta)\boldsymbol{G}_m+\sigma_m^2\boldsymbol{I}\succeq 0, \\ &\qquad\forall\boldsymbol{G}_m\in\mathcal{G}_m,\forall m, && \text{(19b)}\\ &\quad\rho_m\mathrm{tr}(\boldsymbol{G}_m^{\mathrm{H}}\boldsymbol{\varGamma}(\boldsymbol{\mathcal{W}},\boldsymbol{Q})\boldsymbol{G}_m)\ge\eta_m, \\ &\qquad\forall\boldsymbol{G}_m\in\mathcal{G}_m,\forall m, && \text{(19c)}\\ &\quad\mathrm{tr}(\boldsymbol{C}\boldsymbol{\mathcal{W}}+\boldsymbol{Q})\le P_{\mathrm{r}}, && \text{(19d)}\\ &\quad\mathrm{tr}((\boldsymbol{C}\boldsymbol{\mathcal{W}}+\boldsymbol{Q})\boldsymbol{e}_k\boldsymbol{e}_k^{\mathrm{H}})\le P_k,\forall k. && \text{(19e)} \end{aligned}$$

It is highlighted that the problem is still a non-convex problem due to the infinite constraints (19b) and (19c). Next, we transform these constraints into linear matrix inequalities (LMIs).

Now, we deal with constraint (19b). To make constraint (19b) trackable, we first introduce the following lemma:

Lemma 1 (Luo *et al.*, 2004) Let $f(\boldsymbol{X})=\boldsymbol{X}^{\mathrm{H}}\boldsymbol{A}\boldsymbol{X}+\boldsymbol{X}^{\mathrm{H}}\boldsymbol{B}+\boldsymbol{B}^{\mathrm{H}}\boldsymbol{X}+\boldsymbol{C}$ and $\boldsymbol{E}\succeq 0$. Then the implication

$$\mathrm{tr}(\boldsymbol{E}\boldsymbol{X}\boldsymbol{X}^{\mathrm{H}})\le 1\Rightarrow f(\boldsymbol{X})\succeq 0$$

holds if and only if there exists $\mu\ge 0$, such that

$$\begin{bmatrix}\boldsymbol{C} & \boldsymbol{B}^{\mathrm{H}}\\ \boldsymbol{B} & \boldsymbol{A}\end{bmatrix}-\mu\begin{bmatrix}\boldsymbol{I} & \boldsymbol{0}\\ \boldsymbol{0} & -\boldsymbol{E}\end{bmatrix}\succeq 0.$$

Using Lemma 1 w.r.t. $\Delta\boldsymbol{G}_m$ via $\boldsymbol{A}=\boldsymbol{\varPsi}(\boldsymbol{\mathcal{W}},\boldsymbol{Q},\beta)$, $\boldsymbol{B}=\bar{\boldsymbol{G}}_m^{\mathrm{H}}\boldsymbol{\varPsi}(\boldsymbol{\mathcal{W}},\boldsymbol{Q},\beta)$, $\boldsymbol{C}=\bar{\boldsymbol{G}}_m^{\mathrm{H}}\boldsymbol{\varPsi}(\boldsymbol{\mathcal{W}},\boldsymbol{Q},\beta)\bar{\boldsymbol{G}}_m+\sigma_m^2\boldsymbol{I}$, and $\boldsymbol{E}=\varepsilon_m^{-2}\boldsymbol{I}$, we obtain the following LMI:

$$\begin{aligned} &\boldsymbol{\varXi}_m(\boldsymbol{\mathcal{W}},\boldsymbol{Q},\beta,\mu_m)\\ &\triangleq\begin{bmatrix}\bar{\boldsymbol{G}}_m^{\mathrm{H}}\\ \boldsymbol{I}\end{bmatrix}\boldsymbol{\varPsi}(\boldsymbol{\mathcal{W}},\boldsymbol{Q},\beta)\begin{bmatrix}\bar{\boldsymbol{G}}_m & \boldsymbol{I}\end{bmatrix}\\ &\quad+\boldsymbol{D}((\sigma_m^2\boldsymbol{I}-\mu_m\boldsymbol{I}),\mu_m\varepsilon_m^{-2}\boldsymbol{I})\succeq 0. \end{aligned} \tag{20}$$

Now, we deal with constraint (19c), by introducing Lemma 2:

Lemma 2 (S-lemma in Luo *et al.* (2004)) Define function

$$f_j(\boldsymbol{x})=\boldsymbol{x}^{\mathrm{H}}\boldsymbol{A}_j\boldsymbol{x}+2\,\mathrm{Re}\{\boldsymbol{b}_j^{\mathrm{H}}\boldsymbol{x}\}+c_j,\quad j=1,2,\cdots,$$

where $\boldsymbol{A}_j=\boldsymbol{A}_j^{\mathrm{H}}\in\mathbb{C}^{n\times n}$, $\boldsymbol{b}_j\in\mathbb{C}^{n\times 1}$, and $c_j\in\mathbb{R}$. The implication $f_1(\boldsymbol{x})\le 0\Rightarrow f_2(\boldsymbol{x})\le 0$ holds if and only if there exists $\lambda\ge 0$ such that

$$\lambda\begin{bmatrix}\boldsymbol{A}_1 & \boldsymbol{b}_1\\ \boldsymbol{b}_1^{\mathrm{H}} & c_1\end{bmatrix}-\begin{bmatrix}\boldsymbol{A}_2 & \boldsymbol{b}_2\\ \boldsymbol{b}_2^{\mathrm{H}} & c_2\end{bmatrix}\succeq 0,$$

provided that there exists a point $\boldsymbol{x}_0$ such that $f_1(\boldsymbol{x}_0)<0$.

To use Lemma 2 w.r.t. $\Delta\boldsymbol{G}_m$, we denote $\boldsymbol{g}_m\triangleq\mathrm{vec}(\boldsymbol{G}_m)$, $\bar{\boldsymbol{g}}_m\triangleq\mathrm{vec}(\bar{\boldsymbol{G}}_m)$, and $\Delta\boldsymbol{g}_m\triangleq\mathrm{vec}(\Delta\boldsymbol{G}_m)$. It is easy to know that $\|\Delta\boldsymbol{G}_m\|_{\mathrm{F}}\le\varepsilon_m\Leftrightarrow\|\Delta\boldsymbol{g}_m\|\le\varepsilon_m$. Then constraint (19c) can be equivalently rewritten as

$$-\boldsymbol{g}_m^{\mathrm{H}}(\boldsymbol{I}\otimes\boldsymbol{\varGamma}(\boldsymbol{\mathcal{W}},\boldsymbol{Q}))\boldsymbol{g}_m+\eta_m/\rho_m\le 0. \tag{21}$$

To make constraint (21) trackable, using Lemma 2 w.r.t. $\Delta\boldsymbol{g}_m$ via $\boldsymbol{A}_2=-\boldsymbol{I}\otimes\boldsymbol{\varGamma}(\boldsymbol{\mathcal{W}},\boldsymbol{Q})$, $\boldsymbol{b}_2=-\bar{\boldsymbol{g}}_m^{\mathrm{H}}(\boldsymbol{I}\otimes\boldsymbol{\varGamma}(\boldsymbol{\mathcal{W}},\boldsymbol{Q}))$, $c_2=-\bar{\boldsymbol{g}}_m^{\mathrm{H}}(\boldsymbol{I}\otimes\boldsymbol{\varGamma}(\boldsymbol{\mathcal{W}},\boldsymbol{Q}))\bar{\boldsymbol{g}}_m+\eta_m/\rho_m$, $\boldsymbol{A}_1=\boldsymbol{I}$, $\boldsymbol{b}_1=\boldsymbol{0}$, and $c_1=-\varepsilon_m^2$, we obtain the following LMI:

$$\begin{aligned} &\boldsymbol{\varUpsilon}_m(\boldsymbol{\mathcal{W}},\boldsymbol{Q},\theta_m)\\ &\triangleq\begin{bmatrix}\boldsymbol{I}\\ \bar{\boldsymbol{g}}_m^{\mathrm{H}}\end{bmatrix}(\boldsymbol{I}\otimes\boldsymbol{\varGamma}(\boldsymbol{\mathcal{W}},\boldsymbol{Q}))\begin{bmatrix}\boldsymbol{I} & \bar{\boldsymbol{g}}_m\end{bmatrix}\\ &\quad+\boldsymbol{D}(\theta_m\boldsymbol{I},-\theta_m\varepsilon_m^2-\eta_m/\rho_m)\succeq 0. \end{aligned} \tag{22}$$

By taking into account all the relationships, we obtain the following problem:

$$\gamma_{\rm relax}(\beta) \triangleq$$

$$\max_{\substack{\boldsymbol{\mathcal{W}}\succeq 0,\boldsymbol{Q}\succeq 0,\\ \mu_m,\theta_m}} \frac{\mathrm{tr}(\boldsymbol{A}\boldsymbol{\mathcal{W}})}{\beta^{-1}(\sigma_{\rm I}^2+\mathrm{tr}(\boldsymbol{B}\boldsymbol{\mathcal{W}}+\boldsymbol{h}\boldsymbol{h}^{\rm H}\boldsymbol{Q}))} \tag{23a}$$

$$\text{s.t.} \quad \boldsymbol{\varXi}_m(\boldsymbol{\mathcal{W}},\boldsymbol{Q},\beta,\mu_m)\succeq 0, \mu_m\geq 0, \forall m, \tag{23b}$$

$$\boldsymbol{\varUpsilon}_m(\boldsymbol{\mathcal{W}},\boldsymbol{Q},\theta_m)\succeq 0, \theta_m\geq 0, \forall m, \tag{23c}$$

$$\mathrm{tr}(\boldsymbol{C}\boldsymbol{\mathcal{W}}+\boldsymbol{Q})\leq P_{\rm r}, \tag{23d}$$

$$\mathrm{tr}((\boldsymbol{C}\boldsymbol{\mathcal{W}}+\boldsymbol{Q})\boldsymbol{e}_k\boldsymbol{e}_k^{\rm H})\leq P_k, \forall k. \tag{23e}$$

Problem (23) is a quasi-convex problem, which can be turned into a convex problem by employing the Charnes and Cooper transformation (Charnes and Cooper, 1962). Specifically, by introducing a slack variable $\xi > 0$ and making the following change of variables $\tilde{\boldsymbol{\mathcal{W}}} = \xi\boldsymbol{\mathcal{W}}$, $\tilde{\boldsymbol{Q}} = \xi\boldsymbol{Q}$, $\tilde{u}_m = \xi u_m$, and $\tilde{\theta}_m = \xi\theta_m$, problem (23) can be recast as

$$\max_{\tilde{\boldsymbol{\mathcal{W}}}\succeq 0,\tilde{\boldsymbol{Q}}\succeq 0,\xi,\tilde{\mu}_m,\tilde{\theta}_m} \mathrm{tr}(\boldsymbol{A}\tilde{\boldsymbol{\mathcal{W}}}) \tag{24a}$$

$$\text{s.t.} \quad \xi\sigma_{\rm I}^2+\mathrm{tr}(\boldsymbol{B}\tilde{\boldsymbol{\mathcal{W}}}+\boldsymbol{h}\boldsymbol{h}^{\rm H}\tilde{\boldsymbol{Q}})=\beta, \tag{24b}$$

$$\tilde{\boldsymbol{\varXi}}_m(\tilde{\boldsymbol{\mathcal{W}}},\tilde{\boldsymbol{Q}},\beta,\tilde{\mu}_m)\succeq 0, \tilde{\mu}_m\geq 0, \forall m, \tag{24c}$$

$$\tilde{\boldsymbol{\varUpsilon}}_m(\tilde{\boldsymbol{\mathcal{W}}},\tilde{\boldsymbol{Q}},\tilde{\theta}_m)\succeq 0, \tilde{\theta}_m\geq 0, \forall m, \tag{24d}$$

$$\mathrm{tr}(\boldsymbol{C}\tilde{\boldsymbol{\mathcal{W}}}+\tilde{\boldsymbol{Q}})\leq \xi P_{\rm r}, \tag{24e}$$

$$\mathrm{tr}((\boldsymbol{C}\tilde{\boldsymbol{\mathcal{W}}}+\tilde{\boldsymbol{Q}})\boldsymbol{e}_k\boldsymbol{e}_k^{\rm H})\leq \xi P_k, \forall k, \tag{24f}$$

where

$$\tilde{\boldsymbol{\varXi}}_m(\tilde{\boldsymbol{\mathcal{W}}},\tilde{\boldsymbol{Q}},\beta,\tilde{\mu}_m) \triangleq \begin{bmatrix} \bar{\boldsymbol{G}}_m^{\rm H} \\ \boldsymbol{I} \end{bmatrix} \boldsymbol{\varPsi}(\tilde{\boldsymbol{\mathcal{W}}},\tilde{\boldsymbol{Q}},\beta) \begin{bmatrix} \bar{\boldsymbol{G}}_m & \boldsymbol{I} \end{bmatrix} + \boldsymbol{D}((\xi\sigma_m^2\boldsymbol{I}-\tilde{\mu}_m\boldsymbol{I}),\tilde{\mu}_m\varepsilon_m^{-2}\boldsymbol{I})\succeq 0, \tag{25a}$$

$$\tilde{\boldsymbol{\varUpsilon}}_m(\tilde{\boldsymbol{\mathcal{W}}},\tilde{\boldsymbol{Q}},\tilde{\theta}_m) \triangleq \begin{bmatrix} \boldsymbol{I} \\ \bar{\boldsymbol{g}}_m^{\rm H} \end{bmatrix} (\boldsymbol{I}\otimes\boldsymbol{\varGamma}(\tilde{\boldsymbol{\mathcal{W}}},\tilde{\boldsymbol{Q}})) \begin{bmatrix} \boldsymbol{I} & \bar{\boldsymbol{g}}_m \end{bmatrix} + \boldsymbol{D}(\tilde{\theta}_m\boldsymbol{I},-\tilde{\theta}_m\varepsilon_m^2-\xi\eta_m/\rho_m)\succeq 0. \tag{25b}$$

Problem (24) is an SDP problem, which can be efficiently solved by the existing disciplined convex programming toolbox such as CVX (Grant *et al.*, 2005).

To summarize, for a fixed β, it is easy to obtain $\tilde{\boldsymbol{\mathcal{W}}}^\star$ and $\tilde{\boldsymbol{Q}}^\star$. In addition, since $\beta \in [\lambda_{\min}((\boldsymbol{A}+\boldsymbol{B}),\boldsymbol{B}),1]$, the optimal β (i.e., maximizing $\gamma_{\rm relax}(\beta)$ in problem (11)) can be handled by performing a one-dimensional linear search. Once problem (24) is solved, the solution $(\tilde{\boldsymbol{\mathcal{W}}}^\star,\tilde{\boldsymbol{Q}}^\star,\xi^\star)$ can be used to recover $\boldsymbol{\mathcal{W}}^\star$ and $\boldsymbol{Q}^\star$.

Until this, we have proposed an SDR method for problem (12); however, since we have relaxed the non-convex rank-one constraint, one may wonder whether the SDR is tight for problem (12). In what follows, we will discuss the SDR tightness for problem (12).

3.3 SDR tightness for problem (12)

In general, solving SDR problem (23) does not mean solving the original non-convex problem (12), as we have dropped the rank-one constraint in the development of problem (23). However, we will show below that SDR always obtains a rank-one optimal solution to problem (23).

To this end, employing a similar approach as in Yang *et al.* (2013a), we consider the following secrecy rate constrained power minimization problem:

$$\min_{\substack{\boldsymbol{\mathcal{W}}\succeq 0,\boldsymbol{Q}\succeq 0,\\ \mu_m,\theta_m}} \mathrm{tr}(\boldsymbol{C}\boldsymbol{\mathcal{W}}) \tag{26a}$$

$$\text{s.t.} \quad \mathrm{tr}(\boldsymbol{A}\boldsymbol{\mathcal{W}})\geq \frac{\gamma_{\rm relax}(\beta)}{\beta}(\sigma_{\rm I}^2+\mathrm{tr}(\boldsymbol{B}\boldsymbol{\mathcal{W}}+\boldsymbol{h}\boldsymbol{h}^{\rm H}\boldsymbol{Q})), \tag{26b}$$

$$\mathrm{tr}(\boldsymbol{C}\boldsymbol{\mathcal{W}}+\boldsymbol{Q})\leq P_{\rm r}, \tag{26c}$$

$$\mathrm{tr}((\boldsymbol{C}\boldsymbol{\mathcal{W}}+\boldsymbol{Q})\boldsymbol{e}_k\boldsymbol{e}_k^{\rm H})\leq P_k, \forall k, \tag{26d}$$

$$\boldsymbol{\varXi}_m(\boldsymbol{\mathcal{W}},\boldsymbol{Q},\beta,\mu_m)\succeq 0, \mu_m> 0, \forall m, \tag{26e}$$

$$\boldsymbol{\varUpsilon}_m(\boldsymbol{\mathcal{W}},\boldsymbol{Q},\theta_m)\succeq 0, \theta_m> 0, \forall m. \tag{26f}$$

Notice that $\gamma_{\rm relax}(\beta)$ is the optimal value of problem (23), which is now a constraint in problem (26). First we have the following proposition:

Proposition 1 Any feasible solution of problem (26) is optimal for problem (23). The proof is similar to that for Proposition 2 in Yang *et al.* (2013a), and is thus omitted here.

Proposition 2 For $\gamma(\beta) > 0$, any optimal $\boldsymbol{\mathcal{W}}^\star$ to problem (26) always satisfies $\mathrm{rank}(\boldsymbol{\mathcal{W}}^\star) = 1$. The proof for Proposition 2 is given in Appendix.

Proposition 3 Suppose that the original problem (12) is feasible for $\gamma(\beta) > 0$. Then the optimal solution can be obtained by solving SDP problem (26). Furthermore, the optimal solution $\boldsymbol{\mathcal{W}}^\star$ must be of rank one.

Proof Proposition 3 is a direct result of Propositions 1 and 2.

In particular, if SDR obtains a higher-rank solution for problem (23), then we can obtain a rank-one optimal solution by solving the corresponding power minimization problem (26).

4 Simulation results

In this section, we evaluate the performance of our scheme through Monte Carlo simulations. Specifically, we compare the proposed design with the following methods: (1) nonrobust CBAN, e.g., designing the CBAN based on the estimated ERs' CSI; (2) CBAN without considering security, e.g., maximizing IR's achievable information rate while satisfying the ERs' EH constraint, without considering that ERs may eavesdrop the information; (3) robust CB without AN, e.g., the optimal CB vector which can be obtained by solving problem (9) via setting $\boldsymbol{Q}=\boldsymbol{0}$; (4) null-space CBAN, which is a modified version of the null-space CB method in Yang *et al.* (2013a), e.g., completely eliminating the confidential information leaked to all ERs by projecting the signal received onto the null space of the ERs channel, and allowing relays to use part of the power to generate AN. It should be mentioned that the null-space CBAN can be used only in the case where the number of relays is larger than the sum of all the ERs' antennas, which will be further confirmed by the simulation results.

We assume that all the entries of channel responses $\boldsymbol{f}$, $\boldsymbol{h}$, and $\boldsymbol{G}_m$ are independent and identically distributed (i.i.d.) complex Gaussian random variables with zero mean and unit variance. The following parameters $\{K=6,\ N_{\rm e}=2,\ M=2,\ P_{\rm s}=P_{\rm r}=10$ dBW, $P_k=P_{\rm r}/K, \forall\, k,\ \sigma_{\rm r}^2=\sigma_{\rm I}^2=\sigma_m^2=1, \forall\, m\}$ and $\{\rho_m=0.5,\ \eta_m=0$ dBW, $\varepsilon_m=0.1, \forall\, m\}$ are set for the simulation examples unless specified. Our design and the other four designs are labeled as robust CBAN, nonrobust CBAN, CBAN-wo-SE, CB-wo-AN, and null-space CBAN (Yang *et al.*, 2013a), respectively.

4.1 Worst-case secrecy rate versus relay power budget $P_{\rm r}$

Fig. 2 illustrates the worst-case secrecy rates of five different schemes versus the relay power budget $P_{\rm r}$. It is observed from Fig. 2 that our robust CBAN design outperforms the other schemes in the total relay power region, while the CBAN without considering security is the worst design. It should be noted that in the low relay power region, the robust CB without AN scheme outperforms the null-space CBAN scheme, while in the middle relay power region, the robust CB without AN scheme is outperformed by the latter. This is because with the growth of the relay power, the adverse effect of the uncertainty of CSI would scale up and become more prominent to the secrecy rate performance, and the robust CB without AN scheme suffers from more loss than the null-space CBAN scheme, as well as our robust CBAN and the nonrobust CBAN scheme. This phenomenon suggests that AN is an effective method for resisting CSI uncertainty. This conclusion will be confirmed further by the next example. In the high relay power region, however, the worst-case secrecy rates for all the schemes seem to grow slowly, since in this region the power of the transmitter becomes the main bottleneck, which limits the secrecy rate performance.

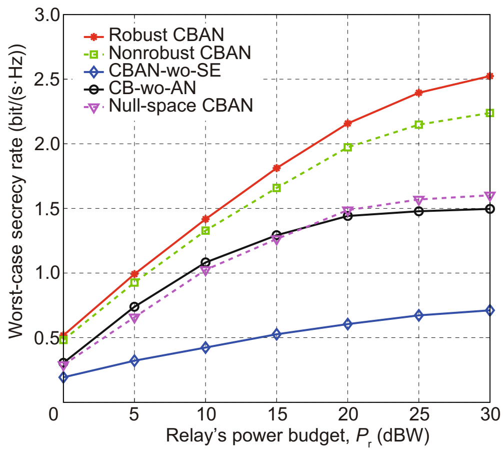

Fig. 2 Worst-case secrecy rate versus the relays' power constraint (CB: cooperative beamforming; AN: artificial noise; CBAN: joint CB and AN; wo: without; SE: security)

4.2 Worst-case secrecy rate versus energy receivers' channel state information uncertainty level φ_m

Fig. 3 shows the worst-case secrecy rates of five different schemes versus the ERS' CSI uncertainty level φ_m. It is observed from Fig. 3 that the worst-case secrecy rates decrease with the increase of φ_m for all the schemes, while our robust CBAN scheme achieves the best performance. In addition, the nonrobust CBAN scheme and the null-space

CBAN scheme obtain higher secrecy rates than the robust CB without AN scheme. Furthermore, the slopes for these schemes which consider AN (including the CBAN without considering security scheme) are smaller than the slope of the robust CB without AN scheme. These observations more clearly illustrate that AN is beneficial in providing robustness.

4.3 Worst-case secrecy rate versus energy harvesting threshold η_m

Fig. 4 shows the worst-case secrecy rates of five different schemes versus the EH threshold η_m. It is seen that the worst-case secrecy rates decrease with the increase of η_m for all the schemes. When the EH threshold is small, the secrecy rates decrease slowly, whereas when the threshold is large, the secrecy rates decrease faster. However, our robust CBAN scheme achieves a better performance than the others. In addition, there is a remarkable phenomenon that for the four schemes which consider AN, the secrecy rates drop quickly when η_m is about 10 dBW, while for the robust CB without AN scheme, the value is about 5 dBW. This phenomenon demonstrates that AN can provide better suitability to the EH threshold in secure SWIPT systems.

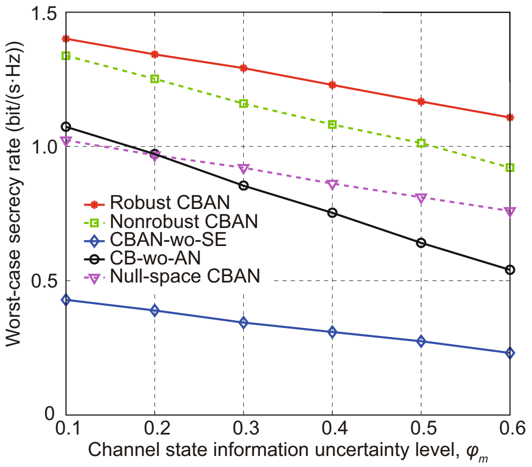

Fig. 3 Worst-case secrecy rate versus the energy receivers' channel state information uncertainty level (CB: cooperative beamforming; AN: artificial noise; CBAN: joint CB and AN; wo: without; SE: security)

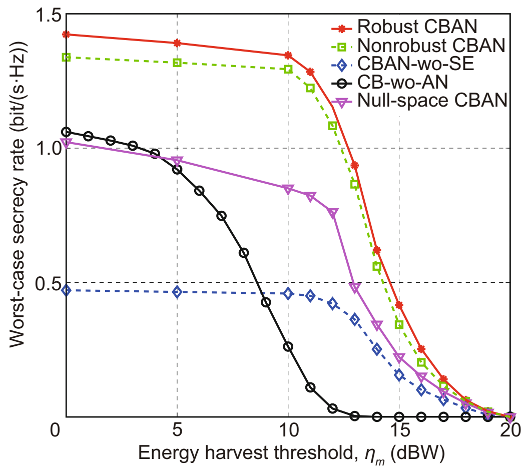

Fig. 4 Worst-case secrecy rate versus the energy harvesting threshold (CB: cooperative beamforming; AN: artificial noise; CBAN: joint CB and AN; wo: without; SE: security)

4.4 Worst-case secrecy rate versus the number of relays K

Fig. 5 plots the worst-case secrecy rates of five different schemes versus the number of relays K. It is seen that the worst-case secrecy rates increase with the increase of K for all the methods due to the increased spatial DoF, while our robust CBAN scheme outperforms other schemes. It should be noted that the null-space CBAN can work only when K is larger than the sum of the numbers of all the ERs' antennas. In this particular example, when $K \leq 4$, the null-space CBAN is invalid since there is no enough DoF left for IR after nulling the ER's channel. In addition, the slope of the null-space CBAN curve is higher than those of other schemes, which suggests that the secrecy rate performance of the null-space CBAN scheme is more sensitive to spatial DoF than those of other schemes.

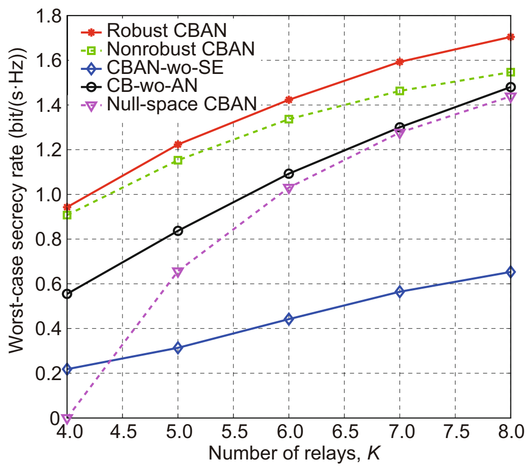

Fig. 5 Worst-case secrecy rate versus the number of relays (CB: cooperative beamforming; AN: artificial noise; CBAN: joint CB and AN; wo: without; SE: security)

4.5 Worst-case secrecy rate versus the number of energy receivers M

Fig. 6 depicts the worst-case secrecy rates of five different schemes versus the number of ERs M. It is seen from the figure that the worst-case secrecy rates decrease with the increase of M for all the methods due to the decreased spatial DoF. Our robust CBAN scheme significantly outperforms the other schemes, especially when M is large. The secrecy rate of the null-space CBAN scheme drops quickly to zero when $M \geq 3$ in this particular example. This further suggests that the spatial DoF has a great influence on the performance of the null-space CBAN scheme.

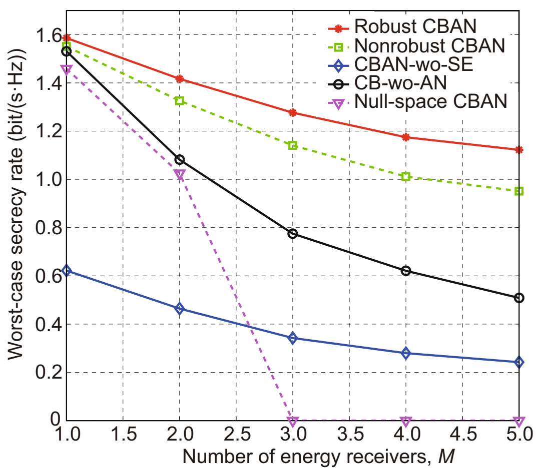

Fig. 6 Worst-case secrecy rate versus the number of energy receivers (CB: cooperative beamforming; AN: artificial noise; CBAN: joint CB and AN; wo: without; SE: security)

4.6 Worst-case secrecy rate versus the number of antennas per energy receiver N_e

Fig. 7 depicts the worst-case secrecy rates of five different schemes versus the number of ERs N_e. Similar to the results in Fig. 6, the worst-case secrecy rates decrease with the increase of N_e for all the methods due to the decreased spatial DoF, while our robust CBAN scheme outperforms the other schemes. Once again, the null-space CBAN scheme becomes invalid when $N_e \geq 3$ in this example. In addition, by comparing Fig. 7 with Fig. 6, we can see that except for the null-space CBAN scheme, the worst-case secrecy rate performances of the other four schemes show approximately linear relationships with N_e in Fig. 7, while in Fig. 6, the decline tendencies of worst-case secrecy rates for these four schemes become weak with the increase of M. This phenomenon suggests that the number of antennas per ER has more influence than the number of ERs on the worst-case secrecy rate, since we consider noncolluding eavesdroppers; thus, the eavesdrop ability of each eavesdropper plays a more important role on the secrecy performance than the number of eavesdroppers.

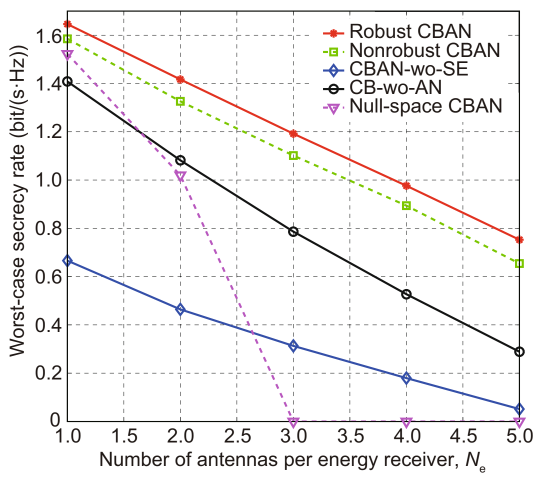

Fig. 7 Worst-case secrecy rate versus the number of antennas per energy receiver (CB: cooperative beamforming; AN: artificial noise; CBAN: joint CB and AN; wo: without; SE: security)

5 Conclusions

In this paper, we have investigated a robust CBAN scheme for secure SWIPT in AF relay networks, in which ERs may act as potential eavesdroppers. To obtain the optimal CB vector and AN covariance, we reformulated the WCSRM problem by using the one-dimensional search based two-level optimization, and established a relationship between the solution to the WCSRM problem and its corresponding power minimization problem. Furthermore, we provided a tightness analysis for this optimization problem, showing that the optimal solution must be of rank one. Simulation results demonstrated the effectiveness of the proposed design.

References

Andrews, J.G., Buzzi, S., Choi, W., *et al.*, 2014. What will 5G be? *IEEE J. Sel. Areas Commun.*, **32**(6):1065-1082. http://dx.doi.org/10.1109/JSAC.2014.2328098

Boyd, S., Vandenberghe, L., 2004. Convex Optimization. Cambridge University Press, Cambridge.

Charnes, A., Cooper, W.W., 1962. Programming with linear fractional functionals. *Nav. Res. Logist.*, **9**(3-4):181-186. http://dx.doi.org/10.1002/nav.3800090303

Chen, X., Ng, D.W.K., Chen, H., 2016. Secrecy wireless information and power transfer: challenges and opportunities. *IEEE Wirel. Commun.*, **23**(2):54-61. http://dx.doi.org/10.1109/MWC.2016.7462485

Chu, Z., Zhu, Z., Hussein, J., 2016. Robust optimization for AN-aided transmission and power splitting for secure MISO SWIPT system. *IEEE Commun. Lett.*, **20**(8):1571-1574. http://dx.doi.org/10.1109/LCOMM.2016.2572684

Feng, R., Li, Q., Zhang, Q., *et al.*, 2015. Robust secure transmission in MISO simultaneous wireless information and power transfer system. *IEEE Trans. Veh. Technol.*, **64**(1):400-405. http://dx.doi.org/10.1109/TVT.2014.2322076

Feng, Y., Yang, Z., Zhu, W.P., *et al.*, 2017. Robust cooperative secure beamforming for simultaneous wireless information and power transfer in amplify-and-forward relay networks. *IEEE Trans. Veh. Technol.*, **66**(3):2354-2366. http://dx.doi.org/10.1109/TVT.2016.2578313

Grant, M., Boyd, S., Ye, Y., 2005. Matlab Software for Disciplined Convex Programming. http://cvxr.com/cvx

Huang, J., Li, Q., Zhang, Q., *et al.*, 2014. Relay beamforming for amplify-and-forward multi-antenna relay networks with energy harvesting constraint. *IEEE Signal Process. Lett.*, **21**(4):454-458. http://dx.doi.org/10.1109/LSP.2014.2305737

Khandaker, M.R.A., Wong, K.K., 2015a. Masked beamforming in the presence of energy-harvesting eavesdroppers. *IEEE Trans. Inform. Forens. Secur.*, **10**(1):40-54. http://dx.doi.org/10.1109/TIFS.2014.2363033

Khandaker, M.R.A., Wong, K.K., 2015b. Robust secrecy beamforming with energy-harvesting eavesdroppers. *IEEE Wirel. Commun. Lett.*, **4**(1):10-13. http://dx.doi.org/10.1109/LWC.2014.2358586

Krikidis, I., Timotheou, S., Nikolaou, S., *et al.*, 2014. Simultaneous wireless information and power transfer in modern communication systems. *IEEE Commun. Mag.*, **52**(11):104-110. http://dx.doi.org/10.1109/MCOM.2014.6957150

Li, J., Petropulu, A.P., Weber, S., 2011. On cooperative relaying schemes for wireless physical layer security. *IEEE Trans. Signal Process.*, **59**(10):4985-4997. http://dx.doi.org/10.1109/TSP.2011.2159598

Li, Q., Zhang, Q., Qin, J., 2014. Secure relay beamforming for simultaneous wireless information and power transfer in nonregenerative relay networks. *IEEE Trans. Veh. Technol.*, **63**(5):2462-2467. http://dx.doi.org/10.1109/TVT.2013.2288318

Li, Q., Yang, Y., Ma, W.K., *et al.*, 2015. Robust cooperative beamforming and artificial noise design for physical-layer secrecy in AF multi-antenna multi-relay networks. *IEEE Trans. Signal Process.*, **63**(1):206-220. http://dx.doi.org/10.1109/TSP.2014.2369001

Li, Q., Zhang, Q., Qin, J., 2016. Secure relay beamforming for SWIPT in amplify-and-forward two-way relay networks. *IEEE Trans. Veh. Technol.*, **65**(11):9006-9019. http://dx.doi.org/10.1109/TVT.2016.2519339

Liu, L., Zhang, R., Chua, K.C., 2013. Secrecy wireless information and power transfer with MISO beamforming. IEEE Global Communications Conf., p.1831-1836. http://dx.doi.org/10.1109/GLOCOM.2013.6831340

Luo, Z.Q., Sturm, J.F., Zhang, S., 2004. Multivariate nonnegative quadratic mappings. *SIAM J. Optim.*, **14**(4):1140-1162. http://dx.doi.org/10.1137/S1052623403421498

Luo, Z.Q., Ma, W.K., So, A.M.C., *et al.*, 2010. Semidefinite relaxation of quadratic optimization problems. *IEEE Signal Process. Mag.*, **27**(3):20-34. http://dx.doi.org/10.1109/MSP.2010.936019

Rodriguez, L.J., Tran, N.H., Duong, T.Q., *et al.*, 2015. Physical layer security in wireless cooperative relay networks: state of the art and beyond. *IEEE Commun. Mag.*, **53**(12):32-39. http://dx.doi.org/10.1109/MCOM.2015.7355563

Salem, A., Hamdi, K.A., Rabie, K.M., 2016. Physical layer security with RF energy harvesting in AF multi-antenna relaying networks. *IEEE Trans. Commun.*, **64**(7):3025-3038. http://dx.doi.org/10.1109/TCOMM.2016.2573829

Shi, Q., Xu, W., Wu, J., *et al.*, 2015. Secure beamforming for MIMO broadcasting with wireless information and power transfer. *IEEE Trans. Wirel. Commun.*, **14**(5):2841-2853. http://dx.doi.org/10.1109/TWC.2015.2395414

Son, P.N., Kong, H.Y., 2015. Cooperative communication with energy-harvesting relays under physical layer security. *IET Commun.*, **9**(17):2131-2139. http://dx.doi.org/10.1049/iet-com.2015.0186

Tian, M., Huang, X., Zhang, Q., *et al.*, 2015. Robust AN-aided secure transmission scheme in MISO channels with simultaneous wireless information and power transfer. *IEEE Signal Process. Lett.*, **22**(6):723-727. http://dx.doi.org/10.1109/LSP.2014.2368695

Wang, C., Wang, H.M., 2015. Robust joint beamforming and jamming for secure AF networks: low-complexity design. *IEEE Trans. Veh. Technol.*, **64**(5):2192-2198. http://dx.doi.org/10.1109/TVT.2014.2334640

Wang, D., Zhang, R., Cheng, X., *et al.*, 2016a. Capacity-enhancing full-duplex relay networks based on power splitting (PS-) SWIPT. *IEEE Trans. Veh. Technol.*, **66**(6):5445-5450. http://dx.doi.org/10.1109/TVT.2016.2616147

Wang, D., Zhang, R., Cheng, X., *et al.*, 2016b. Relay selection in two-way full-duplex energy-harvesting relay networks. IEEE Global Communications Conf., p.1-6. http://dx.doi.org/10.1109/GLOCOM.2016.7842211

Wang, S.H., Wang, B.Y., 2015. Robust secure transmit design in MIMO channels with simultaneous wireless information and power transfer. *IEEE Signal Process. Lett.*, **22**(11):2147-2151. http://dx.doi.org/10.1109/LSP.2015.2464791

Xing, H., Wong, K.K., Nallanathan, A., 2015. Secure wireless energy harvesting-enabled AF-relaying SWIPT networks. IEEE Int. Conf. on Communications, p.2307-2312. http://dx.doi.org/10.1109/ICC.2015.7248669

Xing, H., Liu, L., Zhang, R., 2016. Secrecy wireless information and power transfer in fading wiretap channel. *IEEE Trans. Veh. Technol.*, **65**(1):180-190. http://dx.doi.org/10.1109/TVT.2015.2395725

Xu, J., Liu, L., Zhang, R., 2014. Multiuser MISO beamforming for simultaneous wireless information and power transfer. *IEEE Trans. Signal Process.*, **62**(18):4798-4810. http://dx.doi.org/10.1109/TSP.2014.2340817

Yang, N., Wang, L., Geraci, G., *et al.*, 2015. Safeguarding 5G wireless communication networks using physical layer security. *IEEE Commun. Mag.*, **53**(4):20-27. http://dx.doi.org/10.1109/MCOM.2015.7081071

Yang, Y., Li, Q., Ma, W.K., *et al.*, 2013a. Cooperative secure beamforming for AF relay networks with multiple eavesdroppers. *IEEE Signal Process. Lett.*, **20**(1):35-38. http://dx.doi.org/10.1109/LSP.2012.2227313

Yang, Y., Li, Q., Ma, W.K., *et al.*, 2013b. Optimal joint cooperative beamforming and artificial noise design for secrecy rate maximization in AF relay networks. IEEE 14th Workshop on Signal Processing Advances in Wireless Communications, p.360-364. http://dx.doi.org/10.1109/SPAWC.2013.6612072

Yuen, C., Elkashlan, M., Qian, Y., *et al.*, 2015a. Energy harvesting communications: part 1. *IEEE Commun. Mag.*, **53**(4):68-69. http://dx.doi.org/10.1109/MCOM.2015.7081077

Yuen, C., Elkashlan, M., Qian, Y., *et al.*, 2015b. Energy harvesting communications: part 2. *IEEE Commun. Mag.*, **53**(6):54-55. http://dx.doi.org/10.1109/MCOM.2015.7120017

Yuen, C., Elkashlan, M., Qian, Y., *et al.*, 2015c. Energy harvesting communications: part 3. *IEEE Commun. Mag.*, **53**(8):90-91. http://dx.doi.org/10.1109/MCOM.2015.7180513

Zhang, G., Li, X., Cui, M., *et al.*, 2016. Signal and artificial noise beamforming for secure simultaneous wireless information and power transfer multiple-input multiple-output relaying systems. *IET Commun.*, **10**(7):796-804. http://dx.doi.org/10.1049/iet-com.2015.0482

Zhang, R., Ho, C.K., 2013. MIMO broadcasting for simultaneous wireless information and power transfer. *IEEE Trans. Wirel. Commun.*, **12**(5):1989-2001. http://dx.doi.org/10.1109/TWC.2013.031813.120224

Zhang, R., Song, L., Han, Z., *et al.*, 2012. Physical layer security for two-way untrusted relaying with friendly jammers. *IEEE Trans. Veh. Technol.*, **61**(8):3693-3704. http://dx.doi.org/10.1109/TVT.2012.2209692

Zhang, R., Cheng, X., Yang, L., 2016. Cooperation via spectrum sharing for physical layer security in device-to-device communications underlaying cellular networks. *IEEE Trans. Wirel. Commun.*, **15**(8):5651-5663. http://dx.doi.org/10.1109/TWC.2016.2565579

Zhang, X., 2004. Matrix Analysis and Applications. Tsinghua University Press, Beijing, China (in Chinese).

Appendix: Proof of Proposition 2

Since problem (26) is convex and satisfies the Slater constraint condition, its duality gap is zero and its partial Lagrangian can be defined as

$$\begin{aligned}\mathcal{L}(\mathcal{X}) = {} & \mathrm{tr}(\boldsymbol{C}\boldsymbol{\mathcal{W}}) - \alpha\cdot\mathrm{tr}(\boldsymbol{A}\boldsymbol{\mathcal{W}}) \\ & + \alpha\gamma_{\mathrm{relax}}(\beta)\beta^{-1}(\sigma_{\mathrm{I}}^2 + \mathrm{tr}(\boldsymbol{B}\boldsymbol{\mathcal{W}} + \boldsymbol{h}\boldsymbol{h}^{\mathrm{H}}\boldsymbol{Q})) \\ & + \lambda_0(\mathrm{tr}(\boldsymbol{C}\boldsymbol{\mathcal{W}} + \boldsymbol{Q}) - P_{\mathrm{r}}) \\ & + \sum_{k=1}^{K}\lambda_k(\mathrm{tr}((\boldsymbol{C}\boldsymbol{\mathcal{W}} + \boldsymbol{Q})\boldsymbol{e}_k\boldsymbol{e}_k^{\mathrm{H}}) - P_k) \\ & - \sum_{m=1}^{M}\mathrm{tr}(\boldsymbol{\varOmega}_m\boldsymbol{\varXi}_m) - \sum_{m=1}^{M}\mathrm{tr}(\boldsymbol{T}_m\boldsymbol{\varUpsilon}_m) \\ & - \mathrm{tr}(\boldsymbol{\varPhi}\boldsymbol{\mathcal{W}}) - \mathrm{tr}(\boldsymbol{\varTheta}\boldsymbol{Q}),\end{aligned} \tag{A1}$$

where $\mathcal{X}$ denotes the collection of the primal and dual variables. Specifically, $\alpha\geq 0$, $\lambda_0\geq 0$, $\lambda_k\geq 0$, $\boldsymbol{\varOmega}_m\in\mathbb{H}_+^{N_{\mathrm{e}}+K}$, $\boldsymbol{T}_m\in\mathbb{H}_+^{N_{\mathrm{e}}\times K+1}$, $\boldsymbol{\varPhi}\in\mathbb{H}_+^K$, and $\boldsymbol{\varTheta}\in\mathbb{H}_+^K$ are the Lagrangian multipliers associated with constraints (26b)–(26e) as well as the primal variables $\boldsymbol{\mathcal{W}}$ and $\boldsymbol{Q}$, respectively.

The KKT conditions relevant to the proof are given as follows:

$$\boldsymbol{\varPhi}\boldsymbol{\mathcal{W}} = \boldsymbol{0},\ \boldsymbol{\varTheta}\boldsymbol{Q} = \boldsymbol{0}, \tag{A2a}$$

$$\begin{aligned}\boldsymbol{\varPhi} = {} & \boldsymbol{C} - \alpha\boldsymbol{A} + \frac{\alpha\gamma_{\mathrm{relax}}(\beta)}{\beta}\boldsymbol{B} + \lambda_0\boldsymbol{C} + \boldsymbol{C}\sum_{k=1}^{K}\lambda_k\boldsymbol{e}_k\boldsymbol{e}_k^{\mathrm{H}} \\ & - \sum_{m=1}^{M}\nabla_{\boldsymbol{\mathcal{W}}}\mathrm{tr}(\boldsymbol{\varOmega}_m\boldsymbol{\varXi}_m) - \sum_{m=1}^{M}\nabla_{\boldsymbol{\mathcal{W}}}\mathrm{tr}(\boldsymbol{T}_m\boldsymbol{\varUpsilon}_m),\end{aligned} \tag{A2b}$$

$$\begin{aligned}\boldsymbol{\varTheta} = {} & \frac{\alpha\gamma_{\mathrm{relax}}(\beta)}{\beta}\boldsymbol{h}\boldsymbol{h}^{\mathrm{H}} + \lambda_0\boldsymbol{I} + \sum_{k=1}^{K}\lambda_k\boldsymbol{e}_k\boldsymbol{e}_k^{\mathrm{H}} \\ & - \sum_{m=1}^{M}\nabla_{\boldsymbol{Q}}\mathrm{tr}(\boldsymbol{\varOmega}_m\boldsymbol{\varXi}_m) - \sum_{m=1}^{M}\nabla_{\boldsymbol{Q}}\mathrm{tr}(\boldsymbol{T}_m\boldsymbol{\varUpsilon}_m).\end{aligned} \tag{A2c}$$

Based on the operation of matrix differential in Zhang (2004), we obtain the following relationships:

$$\nabla_{\boldsymbol{Q}}\mathrm{tr}(\boldsymbol{\varOmega}_m\boldsymbol{\varXi}_m) = \boldsymbol{\varPi}_m, \tag{A3a}$$

$$\nabla_{\boldsymbol{\mathcal{W}}}\mathrm{tr}(\boldsymbol{\varOmega}_m\boldsymbol{\varXi}_m) = -\frac{P_{\mathrm{s}}}{\beta^{-1}-1}\boldsymbol{F}^{\mathrm{H}}\boldsymbol{\varPi}_m\boldsymbol{F} + \sigma_{\mathrm{r}}^2\boldsymbol{\varPi}_m\odot\boldsymbol{I}, \tag{A3b}$$

with $\boldsymbol{\varPi}_m = [\bar{\boldsymbol{G}}_m\ \boldsymbol{I}]\boldsymbol{\varOmega}_m[\bar{\boldsymbol{G}}_m\ \boldsymbol{I}]^{\mathrm{H}}$.

Similarly, we obtain

$$\nabla_{\boldsymbol{Q}}\mathrm{tr}(\boldsymbol{T}_m\boldsymbol{\Upsilon}_m)=\sum_{n=1}^{N_\mathrm{e}}\boldsymbol{\Lambda}_m^{(n,n)}, \tag{A4a}$$

$$\nabla_{\boldsymbol{\mathcal{W}}}\mathrm{tr}(\boldsymbol{T}_m\boldsymbol{\Upsilon}_m)=\sigma_\mathrm{r}^2\left(\sum_{n=1}^{N_\mathrm{e}}\boldsymbol{\Lambda}_m^{(n,n)}\right)\odot\boldsymbol{I} + P_\mathrm{s}\boldsymbol{F}^\mathrm{H}\left(\sum_{n=1}^{N_\mathrm{e}}\boldsymbol{\Lambda}_m^{(n,n)}\right)\boldsymbol{F}, \tag{A4b}$$

where $\boldsymbol{\Lambda}_m^{(n,n)}$ are the block submatrices of matrix $[\ \boldsymbol{I}\quad \bar{\boldsymbol{g}}_m\ ]\boldsymbol{T}_m[\ \boldsymbol{I}\quad \bar{\boldsymbol{g}}_m\ ]^\mathrm{H}$, which can be specifically expressed as

$$[\ \boldsymbol{I}\quad \bar{\boldsymbol{g}}_m\ ]\boldsymbol{T}_m[\ \boldsymbol{I}\quad \bar{\boldsymbol{g}}_m\ ]^\mathrm{H} = \begin{bmatrix} \boldsymbol{\Lambda}_m^{(1,1)} & \boldsymbol{\Lambda}_m^{(1,2)} & \cdots & \boldsymbol{\Lambda}_m^{(1,N_\mathrm{e})} \\ \boldsymbol{\Lambda}_m^{(2,1)} & \boldsymbol{\Lambda}_m^{(2,2)} & \cdots & \boldsymbol{\Lambda}_m^{(2,N_\mathrm{e})} \\ \vdots & \vdots & & \vdots \\ \boldsymbol{\Lambda}_m^{(N_\mathrm{e},1)} & \boldsymbol{\Lambda}_m^{(N_\mathrm{e},2)} & \cdots & \boldsymbol{\Lambda}_m^{(N_\mathrm{e},N_\mathrm{e})} \end{bmatrix}. \tag{A5}$$

Multiplying the left side of $\boldsymbol{\Theta}$ by $\boldsymbol{F}^\mathrm{H}$ and the right side by $\boldsymbol{F}$, we obtain

$$\begin{aligned}\boldsymbol{F}^\mathrm{H}\boldsymbol{\Theta}\boldsymbol{F} &= \alpha\gamma_\mathrm{relax}(\beta)\beta^{-1}\boldsymbol{F}^\mathrm{H}\boldsymbol{h}\boldsymbol{h}^\mathrm{H}\boldsymbol{F}+\lambda_0\boldsymbol{F}^\mathrm{H}\boldsymbol{F} \\ &+\boldsymbol{F}^\mathrm{H}\left(\sum_{k=1}^{K}\lambda_k\boldsymbol{e}_k\boldsymbol{e}_k^\mathrm{H}\right)\boldsymbol{F}-\boldsymbol{F}^\mathrm{H}\left(\sum_{m=1}^{M}\boldsymbol{\Pi}_m\right)\boldsymbol{F} \\ &-\boldsymbol{F}^\mathrm{H}\left(\sum_{m=1}^{M}\sum_{n=1}^{N_\mathrm{e}}\boldsymbol{\Lambda}_m^{(n,n)}\right)\boldsymbol{F}.\end{aligned} \tag{A6}$$

Combining these relationships, we can further express $\boldsymbol{\Phi}$ as

$$\begin{aligned}\boldsymbol{\Phi} &= \boldsymbol{C}+\sigma_\mathrm{r}^2(\boldsymbol{\Theta}\odot\boldsymbol{I})-\alpha(1+\gamma_\mathrm{relax}(\beta)\beta^{-1})\boldsymbol{A} \\ &+P_\mathrm{s}\boldsymbol{F}^\mathrm{H}\boldsymbol{\Theta}\boldsymbol{F}+P_\mathrm{s}(1-\beta)^{-1}\boldsymbol{F}^\mathrm{H}\left(\sum_{m=1}^{M}\boldsymbol{\Pi}_m\right)\boldsymbol{F},\end{aligned} \tag{A7}$$

and, together with $\boldsymbol{\Phi}\boldsymbol{\mathcal{W}}=\boldsymbol{0}$, we have

$$\boldsymbol{\mathcal{W}}\boldsymbol{Z}=\alpha(1+\gamma_\mathrm{relax}(\beta)\beta^{-1})\boldsymbol{\mathcal{W}}\boldsymbol{A}, \tag{A8}$$

with

$$\begin{aligned}\boldsymbol{Z} &\triangleq \boldsymbol{C}+\sigma_\mathrm{r}^2(\boldsymbol{\Theta}\odot\boldsymbol{I})+P_\mathrm{s}\boldsymbol{F}^\mathrm{H}\boldsymbol{\Theta}\boldsymbol{F} \\ &+P_\mathrm{s}(1-\beta)^{-1}\boldsymbol{F}^\mathrm{H}\left(\sum_{m=1}^{M}\boldsymbol{\Pi}_m\right)\boldsymbol{F}.\end{aligned} \tag{A9}$$

Since

$$P_\mathrm{s}(1-\beta)^{-1}\boldsymbol{F}^\mathrm{H}\left(\sum_{m=1}^{M}\boldsymbol{\Pi}_m\right)\boldsymbol{F}\succeq 0, \tag{A10}$$

and

$$\sigma_\mathrm{r}^2(\boldsymbol{\Theta}\odot\boldsymbol{I})+P_\mathrm{s}\boldsymbol{F}^\mathrm{H}\boldsymbol{\Theta}\boldsymbol{F}\succeq 0, \tag{A11}$$

we obtain that $\boldsymbol{Z}\succ 0$ has full rank.

In addition, $\mathrm{rank}(\boldsymbol{A})=1$ implies that $\mathrm{rank}(\boldsymbol{\mathcal{W}}) = \mathrm{rank}(\boldsymbol{\mathcal{W}}\boldsymbol{Z}) = \mathrm{rank}(\boldsymbol{\mathcal{W}}\boldsymbol{A}) \leq \mathrm{rank}(\boldsymbol{A}) = 1$, where the first equality is due to full rank of $\boldsymbol{Z}$, the second equality follows Eq. (A8), and the inequality is due to the basic rank inequality $\mathrm{rank}(\boldsymbol{A}\boldsymbol{B}) \leq \min\{\mathrm{rank}(\boldsymbol{A}), \mathrm{rank}(\boldsymbol{B})\}$. Since $\gamma(\beta)>0$ and $\boldsymbol{\mathcal{W}}^\star = \boldsymbol{0}$ cannot be a solution, $\mathrm{rank}(\boldsymbol{\mathcal{W}}^\star)=1$ must hold.